



HAL
open science

Multiple Sliding Surface Control Approach to Twin Rotor MIMO Systems

Quan V. Nguyen, Chang-Ho Hyun

► **To cite this version:**

Quan V. Nguyen, Chang-Ho Hyun. Multiple Sliding Surface Control Approach to Twin Rotor MIMO Systems. *International Journal of Fuzzy Logic and Intelligent Systems*, 2014, 14, pp.171 - 180. <10.5391/IJ-FIS.2014.14.3.171>. <hal-01568848>

HAL Id: hal-01568848

<https://hal.science/hal-01568848v1>

Submitted on 25 Jul 2017

HAL is a multi-disciplinary open access archive for the deposit and dissemination of scientific research documents, whether they are published or not. The documents may come from teaching and research institutions in France or abroad, or from public or private research centers.

L'archive ouverte pluridisciplinaire HAL, est destinée au dépôt et à la diffusion de documents scientifiques de niveau recherche, publiés ou non, émanant des établissements d'enseignement et de recherche français ou étrangers, des laboratoires publics ou privés.



HAL Authorization

Multiple Sliding Surface Control Approach to Twin Rotor MIMO Systems

Quan Nguyen Van and Chang-Ho Hyun

IRS Laboratory, School of Electrical Electronic and Control Engineering, Kongju National University, Cheonan 331-717, Korea



Abstract

In this paper, a multiple sliding surface (MSS) controller for a twin rotor multi-input-multi-output system (TRMS) with mismatched model uncertainties is proposed. The nonlinear terms in the model are regarded as model uncertainties, which do not satisfy the standard matching condition, and an MSS control technique is adopted to overcome them. In order to control the position of the TRMS, the system dynamics are pseudo-decomposed into horizontal and vertical subsystems, and two MSSs are separately designed for each subsystem. The stability of the TRMS with the proposed controller is guaranteed by the Lyapunov stability theory. Some simulation results are given to verify the proposed scheme, and the real time performances of the TRMS with the MSS controller show the effectiveness of the proposed controller.

Keywords: Multiple sliding surface, Mismatched, Model uncertainties, Twin rotor multi-input-multi-output system

1. Introduction

In recent years, there has been an increasing interest in unmanned aerial vehicles (UAVs) in both industrial and academic research. Because of their hover capability, they are useful for many civil missions such as the video supervision of road traffic, surveillance of urban districts, and building inspection for maintenance. Designing the guidance navigation and control algorithms for the autonomous flight of a UAV is a challenging research area because of their nonlinear dynamics and high sensitivity to aerodynamic perturbations.

A twin rotor multi-input-multi-output system (TRMS) is a laboratory prototype of a flight control system, which is a nonlinear multi-input-multi-output (MIMO) system. Because of the similarity of certain aspects of the aero-dynamics of a TRMS and real helicopter-type UAV [1-3], the control of a TRMS has gained much research interest [4-7]. The dynamic modeling and optimal control of a TRMS was presented in [8]. The decoupling control of a TRMS can be found in [9], which used the deadbeat control technique. A novel proportional-integral-derivative (PID) control has been designed to obtain the desired tracking performance [10]. To stabilize the TRMS toward the desired position, a fuzzy logic-based linear quadratic (LQ) regulator controller has been presented [11].

There are two main challenges that must be considered for a TRMS. First, the TRMS is a nonlinear MIMO system. This causes a significant cross-coupling effect between the main rotor and tail rotor. Several studies have been conducted to solve this problem. A multivariable

Received: Sep. 3 2014
Revised : Sep. 19, 2014
Accepted: Sep. 20, 2014

Correspondence to: Chang-Ho Hyun
(hyunch@kongju.ac.kr)
©The Korean Institute of Intelligent Systems

©This is an Open Access article distributed under the terms of the Creative Commons Attribution Non-Commercial License (<http://creativecommons.org/licenses/by-nc/3.0/>) which permits unrestricted non-commercial use, distribution, and reproduction in any medium, provided the original work is properly cited.

nonlinear controller was designed in [12] for the angle control of a TRMS. Based on different linear models, LQ controllers were constructed at different operating points for a similar TRMS in [13].

The second challenge involves the model uncertainties. In order to deal with these highly nonlinear and uncertain systems, the sliding mode control technique, which is conceptually simple and very effective at attenuating the effect of uncertainties, has been considered [14, 15]. However, there are two significant issues with the sliding mode control technique: the chattering problem and matching condition. This control technique uses a discontinuous controller structure, which causes a chattering problem in the control input. In addition, it only works for a class of systems that satisfy the matching conditions, which means uncertainties appear in the same channel as that used for the control input [16]. However, the nonlinear terms in the TRMS model, which are regarded as model uncertainties, do not satisfy this matching condition.

Hence, in this paper, a multiple sliding surface (MSS) controller for the TRMS is proposed to directly counteract the mismatched uncertainties present in the system and simultaneously solve the problem with the highly nonlinear characteristic of the MIMO system. In addition, the chattering problem is attenuated using the nonlinear damping term. Simulation results show that the proposed MSS controller can effectively overcome such problems.

This paper is organized as follows. The non-linear modeling of the TRMS is described in Section 2. In Section 3, the design process for the MSS controller for the TRMS is presented. Section 4 shows the simulation results and the real time performances of the TRMS with the proposed controller. Finally, in Section 5, the main conclusions are summarized, and the future developments are described.

2. Modeling of TRMS

The nonlinear TRMS primarily comprises the main and tail propellers, which are driven by independent main and tail DC motors, respectively. As shown in Figure 1, the propellers are perpendicular to each other and are joined by a beam that can rotate freely in the horizontal and vertical planes, in such a way that its ends move on spherical surfaces. The pitch (yaw) angle can be changed by adjusting the input voltage of the main (tail) motor to control the rotational speed of the main (tail) propeller.

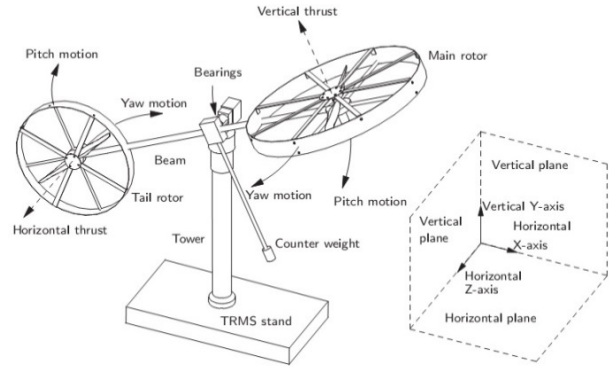


Figure 1. Twin rotor multi-input-multi-output system.

2.1 State Space Model of TRMS

The state space model of the TRMS is described in the following. For the vertical movement, the momentum equation can be derived as follows:

$$I_v \cdot \ddot{\alpha}_v = M_1 - M_{FG} - M_{B\alpha_v} - M_G, \quad (1)$$

where the nonlinear static characteristic

$$M_1 = a_1 \cdot \tau_1^2 + b_1 \cdot \tau_1, \quad (2)$$

the gravity momentum

$$M_{FG} = M_g \cdot \sin \alpha_v, \quad (3)$$

the friction forces momentum

$$M_{B\alpha_v} = B_{1\alpha_v} \cdot \dot{\alpha}_v - \frac{0.0326}{2} \sin 2\alpha_v \cdot \dot{\alpha}_h^2, \quad (4)$$

and the gyroscopic momentum

$$M_G = k_{gy} \cdot M_1 \cdot \dot{\alpha}_h \cdot \cos \alpha_v. \quad (5)$$

The motor and electric control circuit are approximated by a first-order transfer function. Thus, in the Laplace domain, the motor momentum is described by

$$\tau_1 = \frac{k_1}{T_{11}s + T_{10}} \cdot u_v. \quad (6)$$

Similarly, the momentum equation for the horizontal movement is given as

$$I_h \cdot \ddot{\alpha}_h = M_2 - M_{B\alpha_h} - M_R, \quad (7)$$

where the nonlinear static characteristic

$$M_2 = a_2 \cdot \tau_2^2 + b_2 \cdot \tau_2, \quad (8)$$

the friction forces momentum

$$M_{B\alpha_h} = B_{1\alpha_h} \cdot \dot{\alpha}_h, \quad (9)$$

and M_R is the cross-reaction momentum approximated by

$$M_R = \frac{k_c(T_0s + 1)}{(T_p s + 1)} \cdot M_1. \quad (10)$$

The DC motor with the electrical circuit is given by

$$\tau_2 = \frac{k_2}{T_{21}s + T_{20}} \cdot u_h. \quad (11)$$

The complete dynamics of the TRMS system Eqs. (1–11) can be represented in the state space form as follows:

$$\begin{aligned} \frac{d\alpha_v}{dt} &= \dot{\alpha}_v, \\ \frac{d\dot{\alpha}_v}{dt} &= \frac{a_1}{I_v} \tau_1^2 + \frac{b_1}{I_v} \tau_1 - \frac{Mg}{I_v} \sin \alpha_v - \frac{B_{1\alpha_v}}{I_v} \dot{\alpha}_v \\ &\quad + \frac{0.0326}{2I_v} \sin(2\alpha_v) \dot{\alpha}_h^2 - \frac{k_{gy}}{I_v} a_1 \cos(\alpha_v) \dot{\alpha}_h \tau_1^2 \\ &\quad - \frac{k_{gy}}{I_v} b_1 \cos(\alpha_v) \dot{\alpha}_h \tau_1, \\ \frac{d\alpha_h}{dt} &= \dot{\alpha}_h, \\ \frac{d\dot{\alpha}_h}{dt} &= \frac{a_2}{I_h} \tau_2^2 + \frac{b_2}{I_h} \tau_2 \\ &\quad - \frac{B_{1\alpha_h}}{I_h} \dot{\alpha}_h - \frac{k_c a_1}{I_h} 1.75 \tau_1^2 - \frac{1.75}{I_h} k_c b_1 \tau_1, \\ \frac{d\tau_1}{dt} &= -\frac{T_{10}}{T_{11}} \tau_1 + \frac{k_1}{T_{11}} u_v, \\ \frac{d\tau_2}{dt} &= -\frac{T_{20}}{T_{21}} \tau_2 + \frac{k_2}{T_{21}} u_h. \end{aligned} \quad (12)$$

The output is given by

$$y = [\alpha_v \quad \alpha_h]^T,$$

where,

- α_v : pitch (elevation) angle,
- α_h : yaw (azimuth) angle,
- τ_1 : momentum of main rotor,
- τ_2 : momentum of tail rotor.

The system parameters of the TRMS are listed in Table 1.

Table 1. TRMS model parameters

Parameter		Value
I_v	Moment of inertia of vertical rotor	0.068 kg m ²
I_h	Moment of inertia of horizontal rotor	0.02 kg m ²
a_1	Static characteristic	0.0135
b_1	Static characteristic	0.0294
a_2	Static characteristic	0.02
b_2	Static characteristic	0.09
M_g	Gravity momentum	0.32 Nm
$B_{1\alpha_v}$	Friction momentum function	0.006 N-m-s/rad
$B_{1\alpha_h}$	Friction momentum function	0.1 N-m-s/rad
k_{gy}	Gyroscopic momentum parameter	0.05 s/rad
k_1	Main rotor gain	1.1
k_2	Tail rotor gain	0.8
T_{11}	Main rotor denominator	1.1
T_{10}	Main rotor denominator	1
T_{21}	Tail rotor denominator	1
T_{20}	Main rotor denominator	1
T_p	Tail rotor denominator	2
T_0	Tail rotor denominator	3.5

TRMS, twin rotor multi-input-multi-output system.

The state variables can be defined as follows: $x_1 = \alpha_v$ is the pitch angle, $x_3 = \alpha_h$ is the yaw angle, $x_2 = \Omega_v$ is the pitch angular velocity in the vertical plane, $x_4 = \Omega_h$ is the yaw angular velocity in the horizontal plane, $x_5 = \tau_1$ is the momentum of the main motor, and $x_6 = \tau_2$ is the momentum of the tail motor.

The complete state equations of the TRMS can be derived as follows:

$$\begin{aligned} \frac{dx_1}{dt} &= x_2, \\ \frac{dx_2}{dt} &= \frac{a_1}{I_v} x_5^2 + \frac{b_1}{I_v} x_5 - \frac{Mg}{I_v} \sin x_1 - \frac{B_{1\alpha_v}}{I_v} x_2 \\ &\quad + \frac{0.0326}{2I_v} \sin(2x_2) x_4^2 - \frac{k_{gy}}{I_v} a_1 \cos(x_1) x_4 x_5^2 \\ &\quad - \frac{k_{gy}}{I_v} b_1 \cos(x_1) x_4 x_5, \\ \frac{dx_3}{dt} &= x_4, \\ \frac{dx_4}{dt} &= \frac{a_2}{I_h} x_6^2 + \frac{b_2}{I_h} x_6 \\ &\quad - \frac{B_{1\alpha_h}}{I_h} x_4 - \frac{k_c a_1}{I_h} 1.75 x_5^2 - \frac{1.75}{I_h} k_c b_1 x_5, \\ \frac{dx_5}{dt} &= -\frac{T_{10}}{T_{11}} x_5 + \frac{k_1}{T_{11}} u_v, \end{aligned}$$

$$\frac{dx_6}{dt} = -\frac{T_{20}}{T_{21}}x_6 + \frac{k_2}{T_{21}}u_h. \tag{13}$$

2.2 Decomposed Models of TRMS

To simplify the position control complexity, the TRMS is decomposed into a vertical subsystem (TRMS-VS) and horizontal subsystem (TRMS-HS). Using the linearization method, we obtain the linear dynamic system followed by a static nonlinearity.

For the convenience of description, the next symbols are used defined as follows:

$$\begin{aligned} f_1 &= \frac{dx_1}{dt}, & f_2 &= \frac{dx_2}{dt}, & f_3 &= \frac{dx_3}{dt}, \\ f_4 &= \frac{dx_4}{dt}, & f_5 &= \frac{dx_5}{dt}, & f_6 &= \frac{dx_6}{dt}. \end{aligned} \tag{14}$$

The complete state equations of the TRMS are now separated into

$$\begin{aligned} \dot{X}_v &= A_v X_v + B_v u_v + \Delta F_v \\ \dot{X}_h &= A_h X_h + B_h u_h + \Delta F_h \end{aligned} \tag{15}$$

for the TRMS-HS and TRMS-VS, respectively, and

$$X_v = [x_1 \quad x_2 \quad x_5]^T, \quad \Delta F_v = \begin{bmatrix} 0 \\ \Delta F_h(X_v, u_v) \\ 0 \end{bmatrix}, \tag{16}$$

$$X_h = [x_3 \quad x_4 \quad x_6]^T, \quad \Delta F_h = \begin{bmatrix} 0 \\ \Delta F_h(X_h, u_h) \\ 0 \end{bmatrix}, \tag{17}$$

$$\begin{aligned} A_v &= \begin{bmatrix} a_{v11} & a_{v12} & a_{v13} \\ a_{v21} & a_{v22} & a_{v23} \\ a_{v31} & a_{v32} & a_{v33} \end{bmatrix} = \left. \begin{bmatrix} \frac{\partial f_1}{\partial x_1} & \frac{\partial f_1}{\partial x_2} & \frac{\partial f_1}{\partial x_5} \\ \frac{\partial f_2}{\partial x_1} & \frac{\partial f_2}{\partial x_2} & \frac{\partial f_2}{\partial x_5} \\ \frac{\partial f_5}{\partial x_1} & \frac{\partial f_5}{\partial x_2} & \frac{\partial f_5}{\partial x_5} \end{bmatrix} \right|_{X=0} \\ &= \begin{bmatrix} 0 & 1 & 0 \\ \frac{-Mg}{I_v} & \frac{-B_{1\alpha_v}}{I_v} & \frac{b_1}{I_v} \\ 0 & 0 & -\frac{T_{10}}{T_{11}} \end{bmatrix}, \end{aligned} \tag{18}$$

$$\begin{aligned} A_h &= \begin{bmatrix} a_{h11} & a_{h12} & a_{h13} \\ a_{h21} & a_{h22} & a_{h23} \\ a_{h31} & a_{h32} & a_{h33} \end{bmatrix} = \left. \begin{bmatrix} \frac{\partial f_3}{\partial x_3} & \frac{\partial f_3}{\partial x_4} & \frac{\partial f_3}{\partial x_6} \\ \frac{\partial f_4}{\partial x_3} & \frac{\partial f_4}{\partial x_4} & \frac{\partial f_4}{\partial x_6} \\ \frac{\partial f_6}{\partial x_3} & \frac{\partial f_6}{\partial x_4} & \frac{\partial f_6}{\partial x_6} \end{bmatrix} \right|_{X=0} \\ &= \begin{bmatrix} 0 & 1 & 0 \\ 0 & \frac{-B_{1\alpha_h}}{I_h} & \frac{b_2}{I_h} \\ 0 & 0 & -\frac{T_{20}}{T_{21}} \end{bmatrix}, \end{aligned} \tag{19}$$

$$B_v = \begin{bmatrix} b_{v11} \\ b_{v21} \\ b_{v31} \end{bmatrix} = \begin{bmatrix} \frac{\partial f_1}{\partial u_v} \\ \frac{\partial f_2}{\partial u_v} \\ \frac{\partial f_5}{\partial u_v} \end{bmatrix} = \begin{bmatrix} 0 \\ 0 \\ \frac{k_1}{T_{11}} \end{bmatrix}, \tag{20}$$

$$B_h = \begin{bmatrix} b_{h11} \\ b_{h21} \\ b_{h31} \end{bmatrix} = \begin{bmatrix} \frac{\partial f_3}{\partial u_h} \\ \frac{\partial f_4}{\partial u_h} \\ \frac{\partial f_6}{\partial u_h} \end{bmatrix} = \begin{bmatrix} 0 \\ 0 \\ \frac{k_2}{T_{21}} \end{bmatrix}. \tag{21}$$

From Eqs. (12) and (15), we can find the static nonlinear terms in each subsystem plane:

$$\begin{aligned} \Delta f_v(X_v, u_v) &= \frac{a_1}{I_v}x_5^2 + \frac{b_1}{I_v}x_5 - \frac{Mg}{I_v} \sin x_1 - \frac{B_{1\alpha_v}}{I_v}x_2 \\ &\quad + \frac{0.0326}{2I_v} \sin(2x_2)x_4^2 - \frac{k_{gy}}{I_v}a_1 \cos x_1 x_4 x_5^2 \\ &\quad - \frac{k_{gy}}{I_v}b_1 \cos(x_1)x_4 x_5 - a_{v21}x_1 \\ &\quad - a_{v22}x_2 - a_{v23}x_5, \end{aligned} \tag{22}$$

and

$$\begin{aligned} \Delta f_h(X_h, u_h) &= \frac{a_2}{I_h}x_6^2 + \frac{b_2}{I_h}x_6 - \frac{B_{1\alpha_h}}{I_h}x_4 - \frac{k_c a_1}{I_h}1.75x_5^2 \\ &\quad - \frac{1.75}{I_h}k_c b_1 x_5 - a_{h21}x_3 - a_{h22}x_4 - a_{h23}x_6. \end{aligned} \tag{23}$$

3. Design of MSS Controller for TRMS

This section will present the MSS controller design for the TRMS. The nonlinear terms in the model of the TRMS are regarded as mismatched uncertainties, and an MSS control technique is proposed to overcome them. The reaching conditions and stability of the TRMS with the MSS controller will be discussed in this section.

The design procedure for the MSS controller for the TRMS is divided into two tasks. The first task is to design an MSS for the vertical subsystem, and the second is to design an MSS for the horizontal subsystem.

3.1 Design of MSS Controller for Vertical Subsystem

The design of the MSS controller for the position control of the pitch angle is presented in this section.

From Eq. (15), we have the state space equations for the vertical subsystem:

$$\begin{aligned} \dot{x}_1 &= a_{v11}x_1 + a_{v12}x_2 + a_{v13}x_5, \\ \dot{x}_2 &= a_{v21}x_1 + a_{v22}x_2 + a_{v23}x_5 + \Delta f_v, \\ \dot{x}_5 &= a_{v31}x_1 + a_{v32}x_2 + a_{v33}x_5 + b_{v31}u_v \end{aligned} \tag{24}$$

with

$$A_v = \begin{bmatrix} a_{v11} & a_{v12} & a_{v13} \\ a_{v21} & a_{v22} & a_{v23} \\ a_{v31} & a_{v32} & a_{v33} \end{bmatrix} \quad (25)$$

$$= \begin{bmatrix} 0 & 1 & 0 \\ \frac{-Mg}{I_v} & \frac{-B_{1\alpha_v}}{I_v} & \frac{b_1}{I_v} \\ 0 & 0 & -\frac{T_{10}}{T_{11}} \end{bmatrix}.$$

Therefore, we can obtain the reduced equation form of the vertical subsystem as follows:

$$\begin{aligned} \dot{x}_1 &= x_2, \\ \dot{x}_2 &= a_{v21}x_1 + a_{v22}x_2 + a_{v23}x_5 + \Delta f_v, \\ \dot{x}_5 &= a_{v33}x_5 + b_{v31}u_v. \end{aligned} \quad (26)$$

The goal of the controller is to make x_1 track a desired trajectory $x_{1d}(t)$. As Eq. (26) shows, the nonlinear term of the vertical subsystem is under a mismatched condition. Therefore, applying the MSS control to this system, the first sliding surface is defined as follows:

$$S_{1v} = x_1 - x_{1d}. \quad (27)$$

Hence,

$$\dot{S}_{1v} = x_2 - \dot{x}_{1d}. \quad (28)$$

A second sliding surface is defined as follows:

$$S_{2v} = x_2 - x_{2d} \quad (29)$$

$$\dot{S}_{2v} = \dot{x}_2 - \dot{x}_{2d} = a_{v21}x_1 + a_{v22}x_2 + a_{v23}x_5 + \Delta f_v - \dot{x}_{2d}. \quad (30)$$

The synthetic input x_{2d} is chosen to make $S_{1v}\dot{S}_{1v} < 0$. A reasonable choice for x_{2d} is

$$x_{2d} = \dot{x}_{1d} - K_{1v}S_{1v}, \quad (31)$$

where K_{1v} is the first sliding surface gain. Hence,

$$\dot{x}_{2d} = \ddot{x}_{1d} - K_{1v}\dot{S}_{1v}. \quad (32)$$

The third sliding surface is defined as follows:

$$S_{3v} = x_5 - x_{5d}, \quad (33)$$

$$\dot{S}_{3v} = \dot{x}_5 - \dot{x}_{5d} = a_{v33}x_5 + b_{v31}u_v - \dot{x}_{5d}, \quad (34)$$

where the synthetic input x_{5d} is chosen to make $S_{2v}\dot{S}_{2v} < 0$.

A reasonable choice for x_{5d} is

$$\begin{aligned} x_{5d} &= \frac{1}{a_{v23}}(\dot{x}_{2d} - K_{2v}S_{2v} - a_{v21}x_1 - a_{v22}x_2 + \frac{\rho_{1v}^2 S_{2v}}{2\varepsilon_{1v}}), \\ \dot{x}_{5d} &= \frac{1}{a_{v23}}(\ddot{x}_{2d} - K_{2v}\dot{S}_{2v}) \\ &= \frac{1}{a_{v23}} \left\{ [-a_{v21} - a_{v22}(K_{1v} + a_{v22}) - K_{2v}] \dot{S}_{2v} \right. \\ &\quad \left. + \frac{\rho_{1v}^2}{2\varepsilon_{1v}} \right\}. \end{aligned} \quad (35)$$

K_{2v} is the second sliding surface gain. The control input u_v is designed to drive S_{3v} to zero:

$$u_v = \frac{1}{b_{v31}}(\dot{x}_{5d} - K_{3v}S_{3v} - a_{v33}x_5), \quad (37)$$

where K_{3v} in Eq. (37) is the third sliding surface gain.

3.2 Design of MSS Controller for Horizontal Subsystem

This section presents the procedures for designing the MSS controller for the horizontal subsystem. The principle procedures are similar to those shown in the last section.

We have the following state space equations for the horizontal subsystem:

$$\begin{aligned} \dot{x}_3 &= a_{h11}x_3 + a_{h12}x_4 + a_{h13}x_6, \\ \dot{x}_4 &= a_{h21}x_3 + a_{h22}x_4 + a_{h23}x_6 + \Delta f_h, \\ \dot{x}_6 &= a_{h31}x_3 + a_{h32}x_4 + a_{h33}x_6 + b_{h31}u_h \end{aligned} \quad (38)$$

with

$$A_h = \begin{bmatrix} a_{h11} & a_{h12} & a_{h13} \\ a_{h21} & a_{h22} & a_{h23} \\ a_{h31} & a_{h32} & a_{h33} \end{bmatrix} = \begin{bmatrix} 0 & 1 & 0 \\ 0 & \frac{-B_{1\alpha_h}}{I_h} & \frac{b_2}{I_h} \\ 0 & 0 & -\frac{T_{20}}{T_{21}} \end{bmatrix}. \quad (39)$$

Therefore, we can obtain the reduced equation form of the vertical subsystem as follows:

$$\begin{aligned} \dot{x}_3 &= x_4, \\ \dot{x}_4 &= a_{h22}x_4 + a_{h23}x_6 + \Delta f_h, \\ \dot{x}_6 &= a_{h33}x_6 + b_{h31}u_h. \end{aligned} \quad (40)$$

The goal of the controller is to make x_3 track a desired trajectory $x_{3d}(t)$. Applying the MSS control to this system, the first sliding surface is defined as follows:

$$S_{1h} = x_3 - x_{3d}. \quad (41)$$

Hence,

$$\dot{S}_{1h} = x_4 - \dot{x}_{3d}. \tag{42}$$

The second sliding surface is defined as follows:

$$S_{2h} = x_4 - x_{4d}, \tag{43}$$

$$\dot{S}_{2h} = \dot{x}_4 - \dot{x}_{4d} = a_{h22}x_4 + a_{h23}x_6 + \Delta f_h - \dot{x}_{4d}. \tag{44}$$

The synthetic input x_{4d} is chosen to make $S_{1h}\dot{S}_{1h} < 0$. A reasonable choice for x_{4d} is

$$x_{4d} = \dot{x}_{3d} - K_{1h}S_{1h}, \tag{45}$$

where K_{1h} is the first sliding surface gain. Hence,

$$\dot{x}_{4d} = \ddot{x}_{3d} - K_{1h}\dot{S}_{1h}. \tag{46}$$

The third sliding surface is defined as follows:

$$S_{3h} = x_6 - x_{6d}, \tag{47}$$

$$\dot{S}_{3h} = \dot{x}_6 - \dot{x}_{6d} = a_{h33}x_6 + b_{h31}u_h - \dot{x}_{6d}, \tag{48}$$

where the synthetic input x_{6d} is chosen to make $S_{2h}\dot{S}_{2h} < 0$. A reasonable choice for x_{6d} is

$$x_{6d} = \frac{1}{a_{h23}}(\dot{x}_{4d} - K_{2h}S_{2h} - a_{h22}x_4 + \frac{\rho_{2h}^2 S_{2h}}{2\varepsilon_h}), \tag{49}$$

$$\begin{aligned} \dot{x}_{6d} &= \frac{1}{a_{h23}}(\ddot{x}_{4d} - K_{2h}\dot{S}_{2h}) \\ &= \frac{1}{a_{h23}} \left\{ [-a_{h22}^2 + K_{2h}] \dot{S}_{2h} + \frac{\rho_{2h}^2}{2\varepsilon_h} \right\}. \end{aligned} \tag{50}$$

K_{2h} is the second sliding surface gain. The control input u_h is designed to drive S_{3h} to zero:

$$u_h = \frac{1}{b_{h31}}(\dot{x}_{6d} - K_{3h}S_{3h} - a_{h33}x_6), \tag{51}$$

where K_{3h} in Eq. (51) is the third sliding surface gain.

3.3 Stability of TRMS with MSS Controller

The stability of the TRMS with the MSS controller is examined in this section.

3.3.1 Stability of vertical subsystem of TRMS with MSS controller

Theorem 1. If we assume that synthetic inputs x_{2d} and x_{5d} are shown in Eqs. (31) and (35), respectively, and control input

u_v is shown in Eq. (37). Then, the vertical subsystem of the TRMS will be asymptotically stable.

Proof.

Choose a Lyapunov function candidate:

$$V_v = \frac{S_{1v}^2 + S_{2v}^2 + S_{3v}^2}{2} > 0. \tag{52}$$

The derivative of V_v will be

$$\dot{V}_v = S_{1v}\dot{S}_{1v} + S_{2v}\dot{S}_{2v} + S_{3v}\dot{S}_{3v}. \tag{53}$$

Then, with the assumed values of x_{2d} and x_{5d} ,

$$S_{1v}\dot{S}_{1v} + S_{2v}\dot{S}_{2v} < 0. \tag{54}$$

By substituting the value of u_v in Eq. (37) into Eq. (34), we have

$$\begin{aligned} \dot{S}_{3v} &= \dot{x}_5 - \dot{x}_{5d} \\ &= a_{v33}x_5 + b_{v31} \left[\frac{1}{b_{v31}}(\dot{x}_{5d} - K_{3v}S_{3v} - a_{v33}x_5) \right] \\ &\quad - \dot{x}_{5d}, \end{aligned} \tag{55}$$

$$\dot{S}_{3v} = -K_{3v}S_{3v}. \tag{55}$$

Hence, $S_{3v}\dot{S}_{3v} = -K_{3v}S_{3v}^2 < 0$, with $K_{3v} > 0$. When combined with Eq. (54), we have $\dot{V}_v < 0$. Then, we can conclude that the vertical subsystem of the TRMS is asymptotically stable with the MSS controller.

3.3.2 Stability of horizontal subsystem of TRMS with MSS controller

Theorem 2. If we assume that synthetic inputs x_{4d} and x_{6d} are shown in Eqs. (45) and (49), respectively, and control input u_h is shown in Eq. (51), then the horizontal subsystem of the TRMS will be asymptotically stable.

Proof.

Choose a Lyapunov function candidate:

$$V_h = \frac{S_{1h}^2 + S_{2h}^2 + S_{3h}^2}{2} > 0. \tag{56}$$

The derivative of V_h will be

$$\dot{V}_h = S_{1h}\dot{S}_{1h} + S_{2h}\dot{S}_{2h} + S_{3h}\dot{S}_{3h}. \tag{57}$$

Then, with the assumed values of x_{4d} and x_{6d} ,

$$S_{1h}\dot{S}_{1h} + S_{2h}\dot{S}_{2h} < 0. \tag{58}$$

By substituting the value of u_h from Eq. (51) into Eq. (48), we have

$$\begin{aligned} \dot{S}_{3h} &= \dot{x}_6 - \dot{x}_{6d} \\ &= a_{h33}x_6 + b_{h31} \left[\frac{1}{b_{h31}} (\dot{x}_{6d} - K_{3h}S_{3h} - a_{h33}x_6) \right] \\ &\quad - \dot{x}_{6d}, \\ \dot{S}_{3h} &= -K_{3h}S_{3h}. \end{aligned} \tag{59}$$

Hence, $S_{3h}\dot{S}_{3h} = -K_{3h}S_{3h}^2 < 0$, with $K_{3h} > 0$. By combining with Eq. (58), we have $\dot{V}_h < 0$. Then, we can conclude that the horizontal subsystem of the TRMS is asymptotically stable with the MSS controller.

4. Simulation and Experimental Results

The performance of the TRMS controlled by our proposed MSS controller is next investigated in relation to the position control problem.

4.1 Simulation Results

In the MSS controller for the vertical subsystem of the TRMS, the values of the three gains are selected as follows:

$$K_{1v} = 7.5, \quad K_{2v} = 10, \quad K_{3v} = 4.6.$$

In the horizontal subsystem, the values of the three gains are chosen as follows:

$$K_{1h} = 10.5, \quad K_{2h} = 7, \quad K_{3h} = 2.5$$

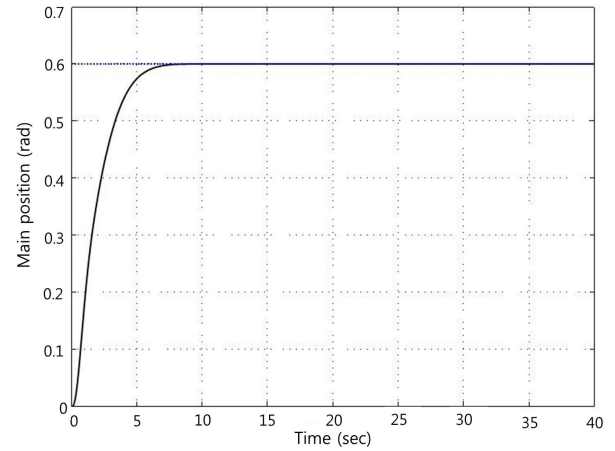
to satisfy the condition mentioned in Section 3.

For the angle tracking, a step function and sinusoidal function are used as the reference commands for the pitch and yaw angles of the TRMS, respectively. The tracking responses depicted in Figures 2 and 3 demonstrate that the MSS controllers are able to track the reference pitch and yaw angles satisfactorily.

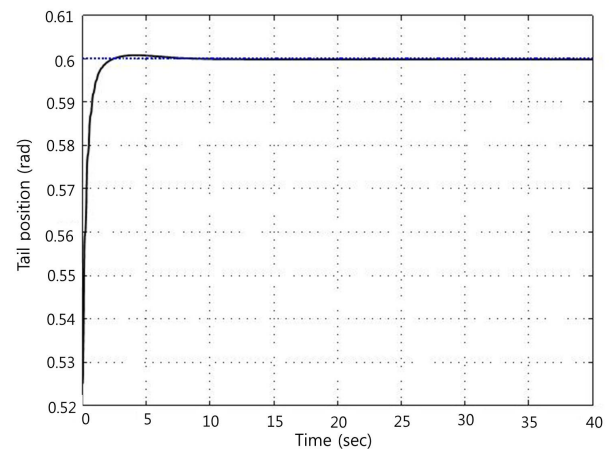
4.2 Experiment Results

The real time performance of the TRMS with the MSS controller will be shown in this section. The TRMS is set up in the laboratory as shown in Figure 4. The controllers are implemented in Windows XP using Simulink, and a proprietary real-time kernel is included with the TRMS system.

The reference signals for the vertical and horizontal parts are fed to the controller, together with the actual position of



(a) Pitch angle



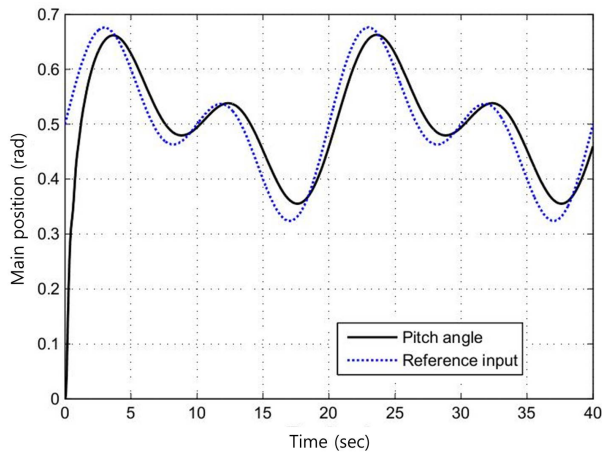
(b) Yaw angle

Figure 2. Step responses of twin rotor multi-input-multi-output system with multiple sliding surface controller. (a) pitch angle and (b) yaw angle.

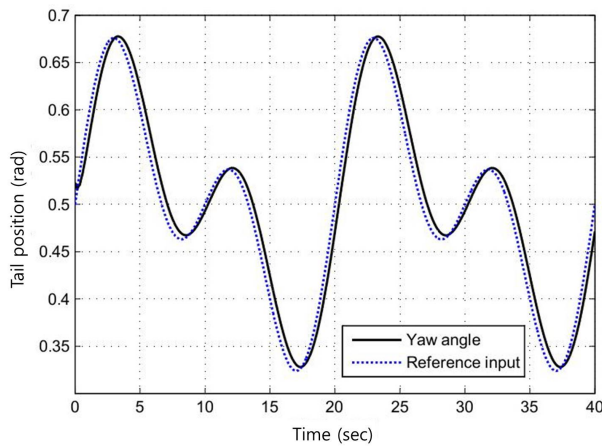
the TRMS. The output from the controller is the voltage to the DC motor and is transformed by the voltage mapping before it is sent to the real-time task, which takes care of all the communication with the TRMS.

The real-time control input signals of the MSS controller for the two rotors of the TRMS are depicted in Figure 5. As can be seen in this figure, the pitch rotor control signal does not have much of a chattering effect, while the tail rotor control signal still has fluctuation, but within an acceptable limit.

In Figure 6, the position tracking performances of the main and tail rotor with the MSS controller are shown. There is not much overshoot and oscillation when these two rotors track the desired position.



(a) Pitch angle



(b) Yaw angle

Figure 3. Sinusoidal responses of twin rotor multi-input-multi-output system with multiple sliding surface controller. (a) pitch angle and (b) yaw angle.

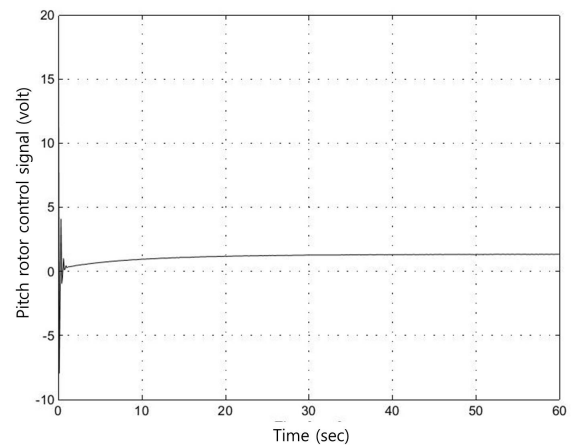
5. Conclusions

In this thesis, an MSS controller was proposed for a nonlinear TRMS with mismatched uncertainties. The stability of the horizontal and vertical subsystems with the MSS controller was guaranteed by the Lyapunov theory. The proposed MSS controller was applied to control the pitch and yaw angles of the TRMS and overcome the mismatched uncertainties. It was observed in the results of both a simulation and experiment that the proposed MSS controller showed effective performance in tracking the desired pitch and yaw angles.

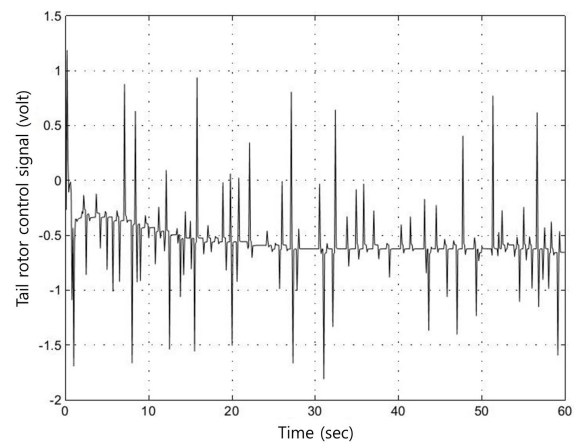
For future development, we can use another robust nonlinear control technique called dynamic surface control (DSC) [17]. The DSC method is basically composed of an MSS and a series



Figure 4. Twin rotor multi-input-multi-output system in laboratory.

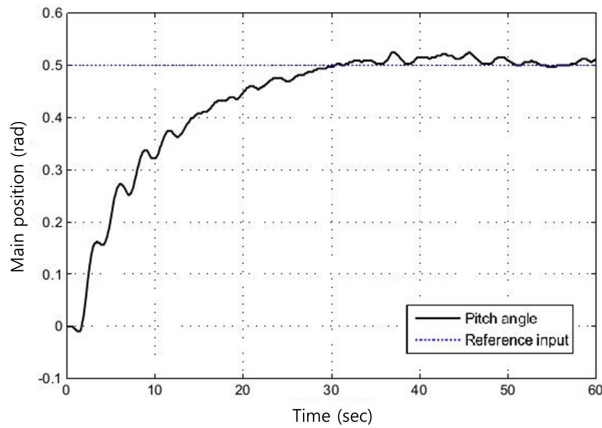


(a) Pitch rotor

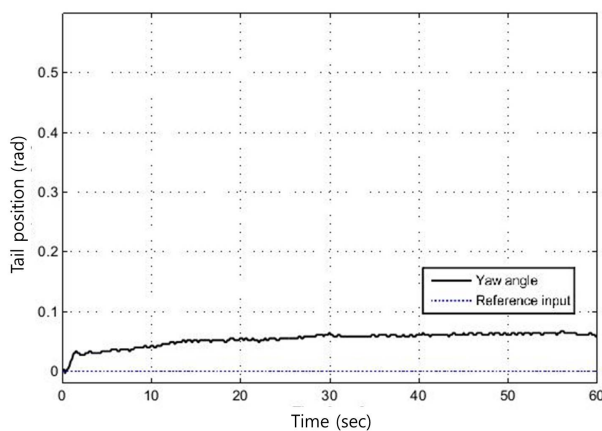


(b) Tail rotor

Figure 5. Real-time control input signals of multiple sliding surface controller. (a) pitch rotor and (b) tail rotor.



(a) Pitch angle



(b) Yaw angle

Figure 6. Real-time step responses of twin rotor multi-input-multi-output system with multiple sliding surface controller. (a) pitch angle and (b) yaw angle.

of first-order low-pass filters. Because of the characteristics of the MSS, DSC avoids the mathematical difficulties of an explosion of terms when obtaining the control input.

Conflict of Interest

No potential conflict of interest relevant to this article was reported.

References

[1] Feedback Instruments, Ltd., *Twin Rotor MIMO System: Advanced Teaching Manual 1 (33-007-4M5)*, Sussex, UK: Feedback Instruments, Ltd., 1997.

[2] F. M. Aldebrez, I. M. Darus, and M. O. Tokhi, “Dynamic modelling of a twin rotor system in hovering position,” in *Proceedings of the 1st International Symposium on Control, Communications and Signal Processing*, Hammamet, Tunisia, March 21-24, 2004, pp. 823-826. <http://dx.doi.org/10.1109/ISCCSP.2004.1296572>

[3] S. M. Ahmad, A. J. Chipperfield, and M. O. Tokhi, “Dynamic modelling and open-loop control of a twin rotor multi-input multi-output system,” in *Proceedings of the Institution of Mechanical Engineers, Part I: Journal of Systems and Control Engineering*, vol. 216, no. 6, pp. 477-496, Sep. 2002. <http://dx.doi.org/10.1177/095965180221600604>

[4] I. Z. M. Darus, F. M. Aldebrez, and M. O. Tokhi, “Parametric modelling of a twin rotor system using genetic algorithms,” in *Proceedings of the 1st International Symposium on Control, Communications and Signal Processing*, Hammamet, Tunisia, March 21-24, 2004, pp. 115-118. <http://dx.doi.org/10.1109/ISCCSP.2004.1296232>

[5] S. M. Ahmad, M. H. Shaheed, A. J. Chipperfield, and M. O. Tokhi, “Nonlinear modelling of a twin rotor MIMO system using radial basis function networks,” in *Proceedings of the IEEE National Aerospace and Electronics Conference*, Dayton, OH, October 12, 2000, pp. 313-320. <http://dx.doi.org/10.1109/NAECON.2000.894926>

[6] J. P. Su, C. Y. Liang, and H. M. Chen, “Robust control of a class of nonlinear systems and its application to a twin rotor MIMO system,” in *Proceedings of the IEEE International Conference on Industrial Technology*, Bangkok, Thailand, December 11-14, 2002, pp. 1272-1277. <http://dx.doi.org/10.1109/ICIT.2002.1189359>

[7] B. U. Islam, N. Ahmed, D. L. Bhatti, and S. Khan, “Controller design using fuzzy logic for a twin rotor MIMO system,” in *Proceedings of the 7th International Multi Topic Conference*, Islamabad, Pakistan, December 8-9, 2003, pp. 264-268. <http://dx.doi.org/10.1109/INMIC.2003.1416722>

[8] S. M. Ahmad, A. J. Chipperfield, and M. O. Tokhi, “Dynamic modeling and optimal control of a twin rotor MIMO system,” in *Proceedings of the IEEE National Aerospace and Electronics Conference*, Dayton, OH, October 12, 2000, pp. 391-398. <http://dx.doi.org/10.1109/NAECON.2000.894937>

- [9] P. Wen and T. W. Lu, "Decoupling control of a twin rotor mimo system using robust deadbeat control technique," *IET Control Theory & Applications*, vol. 2, no. 11, pp. 999-1007, Nov. 2008. <http://dx.doi.org/10.1049/iet-cta:20070335>
- [10] J. G. Juang, M. T. Huang, and W. K. Liu, "PID control using presearched genetic algorithms for a MIMO system," *IEEE Transactions on Systems, Man, and Cybernetics, Part C: Applications and Reviews*, vol. 38, no. 5, pp. 716-727, Sep. 2008. <http://dx.doi.org/10.1109/TSMCC.2008.923890>
- [11] C. W. Tao, J. S. Taur, and Y. C. Chen, "Design of a parallel distributed fuzzy LQR controller for the twin rotor multi-input multi-output system," *Fuzzy Sets and Systems*, vol. 161, no. 15, pp. 2081-2103, Aug. 2010. <http://dx.doi.org/10.1016/j.fss.2009.12.007>
- [12] M. Lopez-Martinez, C. Vivas, and M. G. Ortega, "A multivariable nonlinear H controller for a laboratory helicopter," in *Proceedings of the 44th IEEE Conference on Decision and Control, and European Control Conference*, Seville, Spain, December 15, 2005, pp. 4065-4070. <http://dx.doi.org/10.1109/CDC.2005.1582798>
- [13] T. S. Kim, J. H. Yang, Y. S. Lee, and O. K. Kwon, "Twin rotors system modeling and bumpless transfer implementation algorithm for LQ control," in *Proceedings of the SICE-ICASE International Joint Conference*, Busan, Korea, October 18-21, 2006, pp. 114-119. <http://dx.doi.org/10.1109/SICE.2006.315384>
- [14] M. Won and J. K. Hedrick, "Multiple-surface sliding control of a class of uncertain nonlinear systems," *International Journal of Control*, vol. 64, no. 4, pp. 693-706, Jul. 1996. <http://dx.doi.org/10.1080/00207179608921650>
- [15] S. Mondal and C. Mahanta, "Second order sliding mode controller for twin rotor MIMO system," in *Proceedings of the Annual IEEE India Conference*, Hyderabad, India, December 16-18, 2011, pp. 1-5. <http://dx.doi.org/10.1109/INDCON.2011.6139561>
- [16] D. K. Saroj, I. Kar, and V. K. Pandey, "Sliding mode controller design for Twin Rotor MIMO system with a nonlinear state observer," in *Proceedings of the International Multi-Conference on Automation, Computing, Communication, Control and Compressed Sensing*, Kottayam, India, March 22-23, 2013, pp. 668-673. <http://dx.doi.org/10.1109/iMac4s.2013.6526493>
- [17] D. Swaroop, J. C. Gerdes, P. P. Yip, and J. K. Hedrick, *Dynamic Surface Control of Nonlinear Systems (Technical Report)*, Berkeley, CA: Vehicle Dynamics and Control Laboratory, University of California, 1996.



Nguyen Van Quan received the B.S. degrees in mechatronics engineering from Hanoi University of Science and Technology, Hanoi, Vietnam, in 2011 and he currently takes a master degree course in department of electrical electronic and control engineering, Kongju National University, Korea. His current research interests include automatic guided vehicles, robotics and nonlinear control.



Chang-Ho Hyun received the B.S. degrees in control and instrumentation engineering from Kwangwoon University, Seoul, Korea and the M.S. and Ph.D. degrees in electrical and electronic engineering from Yonsei University, Seoul, Korea in 1999, 2002, 2008.

From 2008 to 2009, he was a senior engineering in Samsung Electronics. He is currently a assistant professor of the School of Electrical, Electronic and Control Engineering at Kongju National University. His current research interests include intelligent control and application, nonlinear control, robotics, mobile robots.